Journal of Crystal Growth 312 (2010) 1334–1339

Contents lists available at ScienceDirect

Journal of Crystal Growth

journal homepage: www.elsevier.com/locate/jcrysgro

Factors influencing the purity of electronic grade phosphine delivered to MOCVD tools

Jun Feng, Mitch Owens, Mark W. Raynor*

Advanced Technology Center, Matheson Tri-Gas Inc., 1861 Lefthand Circle, Longmont, Colorado 80501, USA

ARTICLE INFO

Available online 18 November 2009

Keywords:
A1. Impurities
A1. Low temperature photoluminescence
A1. Mobility
A3. Metalorganic chemical vapor deposition
B1. Phosphine
B2. Indium phosphide

ABSTRACT

Increasing mobility of InP films with usage time of one PH_3 cylinder prompted an investigation into factors influencing the purity of delivered PH_3. The presence of hygroscopic H_xPO_y residues in a delivery system greatly increases the dry-down time compared to that of a clean system. Static delivery system tests show increasing H_2O concentration with time and twice the increase in PH_3 versus N_2 over 48 h indicating reaction of metal oxides in components with PH_3 to generate H_2O. Gas purity may also vary during cylinder usage. Depletion of a high-purity PH_3 cylinder shows consistently low gas phase H_2O levels before phase-break but increasing levels after phase-break, as the cylinder depressurizes. The results highlight the importance of using pure PH_3, employing rigorous cycle-purging procedures to prevent H_xPO_y contamination, switching out cylinders in good time and using purification technology to control H_2O.

1. Introduction

Minimizing incorporation of impurities such as oxygen can be critical to the performance of III–V compound semiconductor devices [1–3]. Oxygen is readily captured from the environment by aluminum and forms deep recombination centers in Al-containing materials [4]. Although it incorporates less in non-Al-containing materials such as InP, effects are still observed. Munns and coworkers reported a significant influence of hydride gas purity on InP. Increased mobility (77 K) was observed as H_2O was decreased from 2 μmol mol^{-1} (ppm) to 100 nmol mol^{-1} (ppb) level in the PH_3 source [5], but the mechanism for this is unclear. In molecular beam epitaxial growth of InP, oxygen can be bound to Be acceptors and to a lesser extent to Si donors [6,7]. Further, in vapor phase epitaxial InP, Iwata and Inoshita [8] have reported that oxygen suppresses Si incorporation. Since Si is the main residual background n-dopant in InP, oxygen may affect Si dopant levels and hence the film properties. Consequently, control of oxygenated impurities such as H_2O in gases such as PH_3 is very important.

PH_3 gas is the most commonly used phosphorus source for InP and associated alloys and is manufactured to a 99.9999% purity level. However, even though the gas purity is confirmed with state-of-the-art instrumentation [9–11], there are many factors that may still influence device performance. Ultimately, device growth and performance tests such as low temperature photoluminescence (PL) and Hall mobility are used to provide complementary information that relate the atomic composition to critical parameters such as gas purity. In this paper we present PL results of InP films grown with high and lower purity PH_3 and data that show increasing mobility of InP films with run time, for growth with the same PH_3 cylinder. This prompted an investigation of factors that influence the purity of PH_3 delivered to MOCVD tools, particularly with respect to H_2O impurity. Issues such as the influence of H_xPO_y contamination in the delivery system on H_2O levels, generation of H_2O as a result of reaction of PH_3 with metal oxides in stagnant lines, and variable H_2O in the PH_3 delivered from cylinders are considered. Point-of-use purification for H_2O control upstream of the MOCVD tool is also discussed.

2. Experiments

2.1. InP MOCVD, mobility and low temperature PL measurements

9 μm InP films were grown using trimethyl-indium (TMI, Optograde, Dow Chemical, Andover, MA) and two PH_3 cylinders (Matheson Tri-Gas, New Johnsonville, TN). Cylinders 1 and 2 contained PH_3 with 99.9999% and 99.9997% purity, respectively, based on gas chromatography and cavity ring-down spectroscopy (CRDS) analysis. MOCVD was performed in a vertical quartz reactor at 10.13 kPa and 650 °C. The PH_3 flow rate was

* Corresponding author. Tel.: +1 303 6780700; fax: +1 303 4420711.
E-mail address: mraynor@matheson-trigas.com (M.W. Raynor).

0022-0248/$ - see front matter © 2009 Elsevier B.V. All rights reserved.
doi:10.1016/j.jcrysgro.2009.11.012

300 sccm, the V/III ratio 300, and the growth rate 11 Å s^{-1}. The substrates were semi-insulating InP oriented approximately 2° off (1 0 0) towards a (1 1 0) direction. Prior to the sequence of InP growths, the MOCVD tool was routinely cleaned and its performance confirmed with a control PH_3 source. After cylinder installation the connection line was cycle purged before initiating the flow of PH_3. For each PH_3 cylinder, two InP layers were grown successively; growths were performed with Cylinder 1, then Cylinder 2. Between the first and second growths, the PH_3 cylinder was kept connected in line. Hall mobility of InP layers were measured at 77 and 300 K [12]. The measuring error of the Hall coefficient was estimated to be $\pm 4\%$. PL measurements were made on the second of the two InP growths from each of the two cylinders, at a temperature of 10 K and using a He–Ne laser at 633 nm and an excitation power of 2 W cm^2.

2.2. H_xPO_y contamination

Cylinder 2 was analyzed multiple times using the CRDS method in [9] to investigate the behavior of H_2O in the PH_3 delivered through the cylinder valve (Fig. 1A). The wet-up and dry-down of a clean and contaminated sampling manifold (Fig. 1B), was also compared. PH_3 containing 2.6 μmol mol^{-1} H_2O or <9 nmol mol^{-1} H_2O was sequentially introduced into the manifold via by-pass or purifier (Nanochem PHX, Matheson Tri-Gas, Longmont, CO) and CRDS was used to measure how rapidly the H_2O level equilibrated.

2.3. SEM study of intentionally generated H_xPO_y contamination

A 316 L stainless steel (SS) sub-manifold was designed to generate H_xPO_y (Fig. 1C). The entire manifold was initially purged with N_2 and then valves V_p and V_m were closed and V_s was opened to let air (atmospheric pressure) fill the second half of the tubing (90 cm × 6.25 mm outside diameter). Valve V_s was then closed and V_p was opened to allow PH_3 gas at 40 psig to fill the first half of the tubing (also 90 cm × 6.25 mm outside diameter). The cylinder valve and V_p were then closed and V_m was opened to let PH_3 and air mix and react for 10 min in the second half of the tube. The procedure was repeated twice more and after purging, the tubing was removed and sectioned. Samples were stored in a N_2 atmosphere to minimize exposure to atmosphere and were analyzed the same day on a JEOL model JSM-7000F scanning electron microscope (SEM-EDS).

2.4. Water measurements with static manifold/analyzer conditions

To study potential H_2O generation from the reaction of PH_3 with metal oxides, purified N_2 at 200 sccm was used to dry down the SS delivery system and CRDS analyzer in Fig. 1A to single digit nmol mol^{-1} levels. The whole system was then closed and left under static conditions for ~2 days and the H_2O concentration monitored. The manifold was then dried down again with purified N_2 and the same experiment repeated with purified PH_3.

2.5. Phosphine cylinder depletion

The set-up shown in Fig. 1A was used to track the gas phase H_2O level during depletion of a PH_3 cylinder until empty. The full cylinder contained 16.33 kg Ultima 6 N purity PH_3.

3. Results and discussion

3.1. Low temperature photoluminescence of MOCVD InP

Table 1 shows the impurity profiles of the two PH_3 cylinders. PL measurements were performed to further confirm the gas purities since all impurities except for N_2 and H_2O were below the detection limit of the gas analysis methods. The PL spectrum of InP is strongly temperature dependent [13,14]. We selected 10 K for comparing the exciton spectra of InP films because at this temperature, high-purity n-type InP exhibits significant upper and lower polariton branches of the free exciton. InP grown from PH_3 Cylinder 1 shows a typical exciton spectrum of high-purity

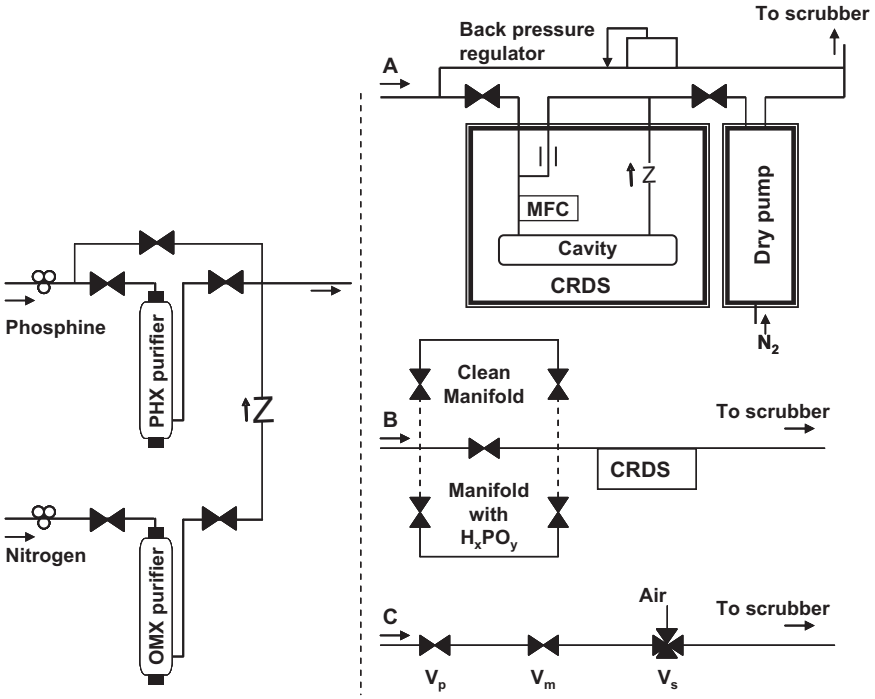

Fig. 1. Diagram of experimental set-up for (A) H_2O analysis and depletion, (B) delivery system contamination and (C) H_xPO_y generation studies.

Table 1
Impurity concentrations in PH_3 Cylinders 1 and 2.

Cylinder no.	Purity (%)	Gas Phase Impurity (nmol mol^{-1})										
		CO_2	CO	O_2	CH_4	N_2	Ar	H_2S	AsH_3	GeH_4	SiH_4	H_2O
1	> 99.9999	< 16	< 14	< 14	< 7	27	< 9	< 15	< 3	< 0.6	< 4	< 50
2	> 99.9997	< 16	< 14	< 14	< 7	63	< 9	< 15	< 3	< 0.6	< 4	180

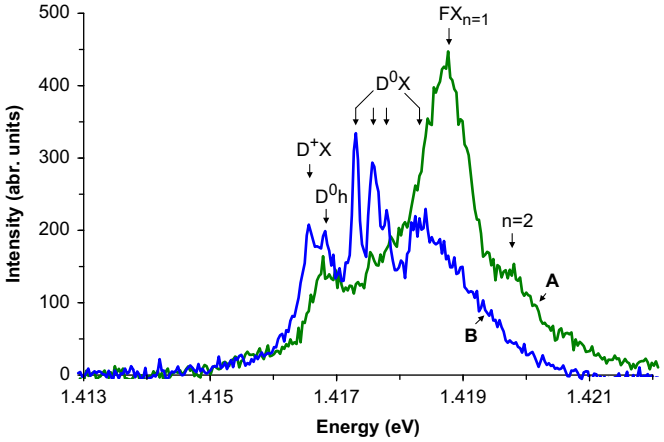

Fig. 2. Low temperature PL of InP grown with PH_3 Cylinder 1 (A) and Cylinder 2 (B); excitation wavelength 633 nm; excitation power 2 mW.

InP (curve A in Fig. 2). The upper ($h\nu_c$(FX)=1.41848 eV) and lower ($h\nu_c$(FX$_{n=2}$)=1.41974 eV) polariton branches of the free exciton are clearly observable, indicating high-purity n-type InP. At this temperature, the radiative decay of free holes with electrons bound to neutral donors ($h\nu_c(D^\circ h)$=1.41661 eV) is clearly visible while the radiative decay lines of neutral donor-bound excitons ($h\nu_c(D^\circ X)_n$ from 1.41692 to 1.41784 eV) are very weak. In the PL spectrum of InP grown from PH_3 Cylinder 2 (curve B in Fig. 2), the first evidence of high-purity InP (the line of lower polariton branch of the free exciton) disappears. Further, the upper polariton branch is not visible because of the higher intensity of $(D^\circ X)_n$. A new line appears for the radiative decay of an exciton bound to an ionized donor (D^+X), while the four ($D^\circ X$) lines are clearly visible compared with the PL profile of high-purity InP at the same low temperature. Clearly, compared to curve B, curve A in Fig. 2 shows a high-purity InP, indicating that Cylinder 1 contains PH_3 of higher purity than Cylinder 2.

3.2. Mobility of InP

In *P* mobility, especially at low temperature, is closely related to the purity of PH_3 at high V/III ratios. With high-purity PH_3, the average mobility of InP films grown under optimized conditions at 580–600 °C and V/III ratio of 450–800 (77 K) is 171,000 cm^2(V s)$^{-1}$. The highest mobility reported in the literature is 234,000 cm^2(V s)$^{-1}$ using high-purity PH_3 and TMI [15]. For typical n-type InP with a mobility of > 100,000 cm^2(V s)$^{-1}$ the carrier concentration is about 10^{14} cm^{-3}. Normally, as the mobility increases, the net carrier concentration (N_D–N_A) decreases, indicating that electrons are the dominant carriers. Table 2 shows the mobility of InP films grown with a V/III ratio of 300, using the two PH_3 cylinders. In particular we noted that the mobility increased significantly with the MOCVD run times. The mobility increases were 12% from run 1 to run 2 for Cylinder 1 and 25% from run 1 to run 2 for Cylinder 2. Similar trends, with mobility increases up to 36%, have been

Table 2
Mobility of InP layers grown in duplicate from Cylinders 1 and 2.

Cylinder	Growth	Mobility (cm^2/V s)		Carrier conc. (cm^{-3})/10E14	
		77 K	300 K	77 K	300 K
Cylinder 1	1st run	137,000	4200	2.12	2.85
	2nd run	153,000	4600	1.53	2.12
Mobility increase (%)		11.68	9.52		
Cylinder 2	1st run	114,000	4100	3.98	4.74
	2nd run	143,000	4300	2.76	2.93
Mobility increase (%)		25.44	4.88		

observed with other similar high-purity PH_3 cylinders. As there are many factors that can influence the purity of layers, the exact cause of the increased mobility in the second run from each cylinder is unclear. However, since the tool performance was verified by running a PH_3 control prior to running the sample cylinders, the observation may be linked directly or indirectly to progressively decreasing H_2O concentration as PH_3 is flowed over time through the delivery system, as discussed in the following sections. Results in Ref. [5], showing the effect of H_2O impurity in PH_3 on mobility of InP, support our inferences in this regard.

3.3. Phosphorus oxide/oxyacid formation and characterization

Factors that can influence the delivery of high-purity gases have been discussed previously [16,17]. For PH_3, cylinder connection or disconnection cycle purge techniques are extremely important, because if not undertaken correctly, traces of air can remain and then react with PH_3 to form solid residues in the delivery system. Previous studies indicate that the residue is a mixture of lower oxides and oxyacids of phosphorus such as H_3PO, H_2PO, HPO, PO and PO_2 intermediates [18] that can go on to form hypophosphorous, phosphorous and phosphoric acids [19]. However, the presence and effects of these contaminants in gas delivery systems has not been discussed in detail in the literature.

To mimic what happens in an incompletely purged delivery line, PH_3 at 40 psig was intentionally introduced into a SS tube that contained air at atmospheric pressure. After removing any residual PH_3, the deposited H_xPO_y residues were analyzed by SEM-EDS (Fig. 3). The yellow colored residue in Fig. 3A had a composition of PO_2 based on EDS (data for H could not be measured), was polycrystalline in nature and had a high density and surface area. The average size of the particles on the surface of the layer was about 0.5 μm. A red-brown residue, with a composition PO, was also formed on a steel rod (Fig. 3B) inserted into the delivery tubing. The SEM image shows this material also had a high porosity and surface area. The two deposits are chemically and structurally different probably because of the different locations of each sample in the tube and how the reaction took place. The rod was positioned farthest from where the PH_3 entered the tube, whereas the yellow deposit was taken from the inside wall of the tube closest to the point of

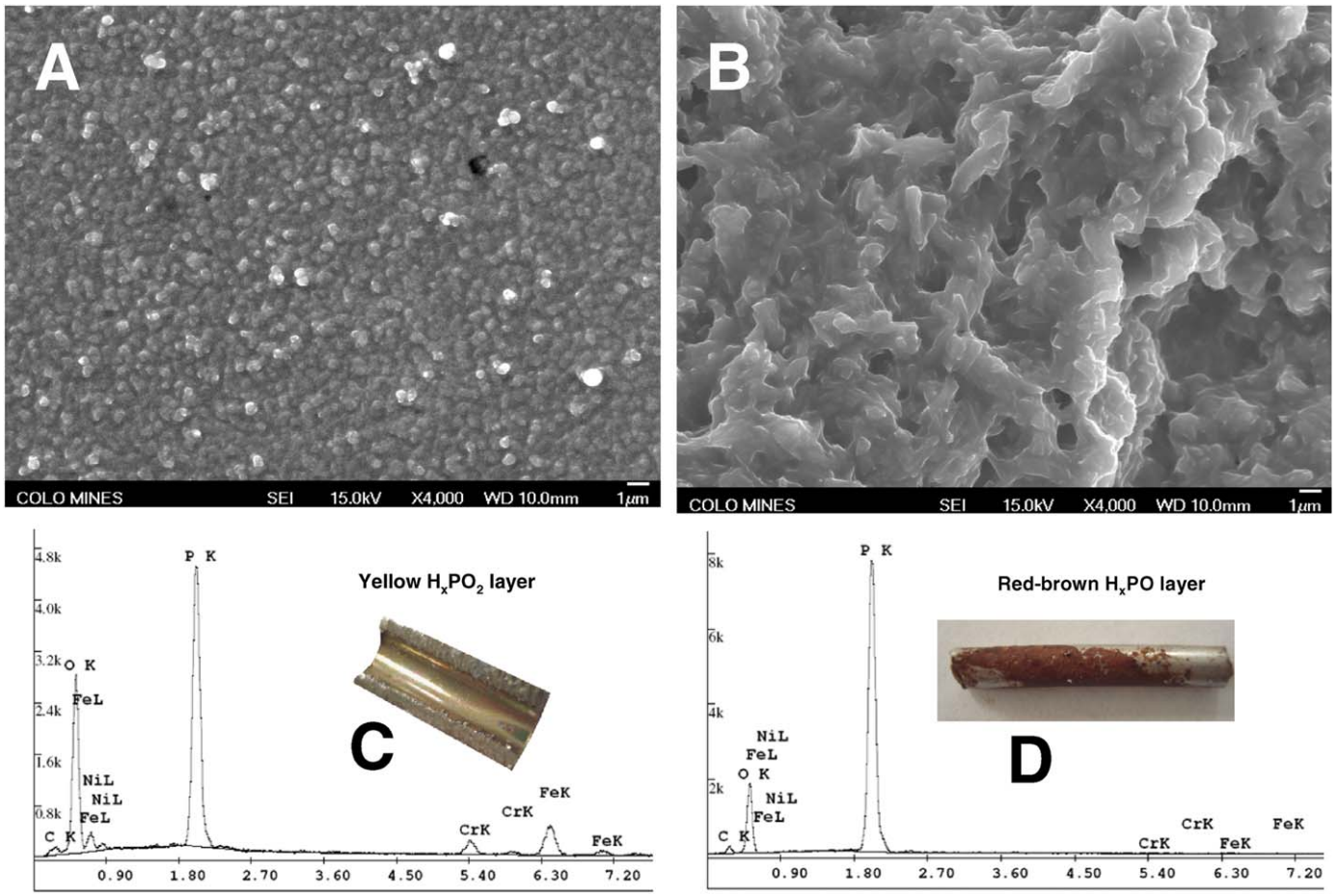

Fig. 3. SEM image of yellow H_xPO_2 on inner tube surface (A) with EDS analysis (C) and photograph (inset); SEM image of red-brown H_xPO on steel rod (B) with EDS analysis (D) and photograph (inset).

entry of the PH_3. The higher oxygen content of the yellow deposit indicates that the PH_3 quenched much of the O_2 as it entered the second tube. Interestingly, although the samples were kept in a N_2 atmosphere, when the red-brown sample was loaded into the SEM vacuum chamber for analysis, the SEM shut down because the chamber pressure criterion could not be met. This indicates that the residue outgassed large amounts of H_2O and is evidence of the hygroscopic nature of H_xPO_y contamination.

3.4. *Effect of H_xPO_y on PH_3 cylinder valve and delivery system*

We studied the water vapor behavior of PH_3 Cylinder 2, which was returned from the field after observing the mobility increase discussed above. After routine cycle-purging of the cylinder connection and sampling manifold, over 3 μmol mol^{-1} H_2O was detected in the PH_3, the first time it was analyzed. The cylinder was kept connected in-line with the cylinder valve closed and the entire sampling system was purged with purified N_2 for over 24 h. When PH_3 was flowed again from the cylinder a second time, the H_2O had decreased but was still ~500 nmol mol^{-1}. After a further 24 and 48 h of purging the cylinder fittings and the delivery system with purified N_2, water measurements from the PH_3 cylinder were close to the original concentration of 180 nmol mol^{-1} (Fig. 4). The slow H_2O dry-down was attributed to H_xPO_y contamination in the cylinder valve. Therefore, even though the gas in the cylinder may meet the H_2O specification, if the cylinder valve contains H_xPO_y residues, dry-down times can be extensive and H_2O in the delivered PH_3 may be elevated for some time and affect devices.

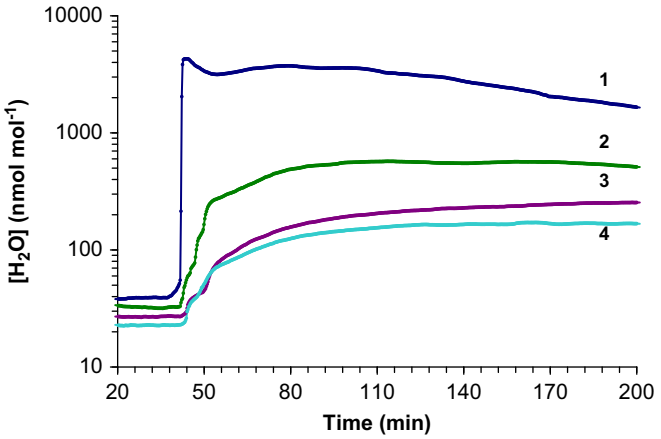

Fig. 4. H_2O concentration during sequential analysis of PH_3 Cylinder 2.

Fig. 5 compares the wet-up and dry-down characteristics of a clean PH_3 delivery system and a system contaminated with H_xPO_y. Curve A in Fig. 5 shows the rapid H_2O equilibration in the clean delivery line when the H_2O level in the PH_3 was changed by passing the PH_3 through the purifier or purifier bypass line. The dry-down time to reach 95% of the final water concentration from 2500 to 100 nmol mol^{-1} was about 20 min. In contrast, curve B in Fig. 5 shows a very slowly equilibrating H_2O profile in a contaminated line, taking over 230 min to reach 95% of the final H_2O concentration.

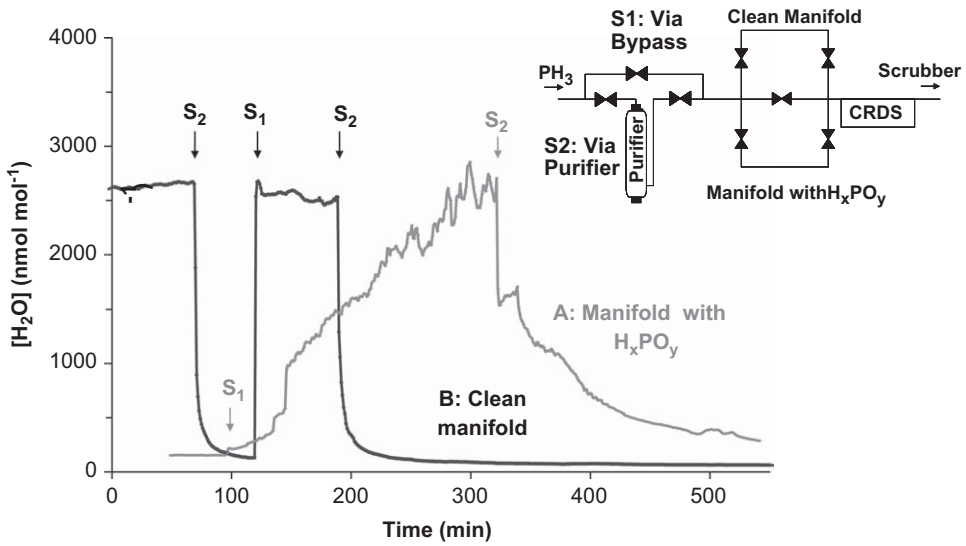

Fig. 5. Wet-up and dry-down trend of manifolds with (A) and without (B) H_xPO_y contamination. In each case wet and dry PH_3 was flowed through the manifolds. S1 and S2 are the points at which PH_3 is switched via purifier bypass and PHX purifier, respectively.

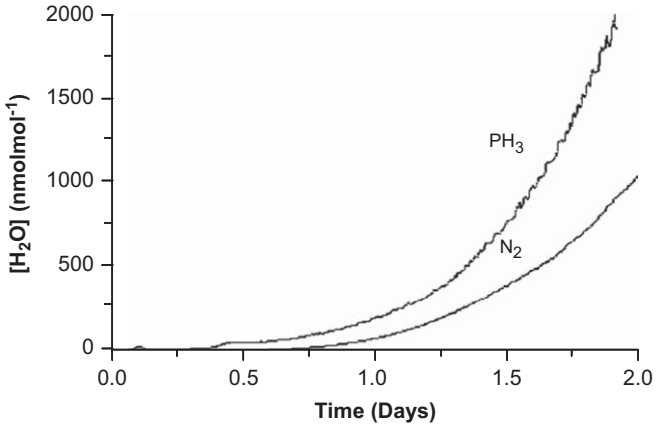

Fig. 6. H_2O concentration increase in PH_3 and N_2 under stagnant conditions over the course of several days.

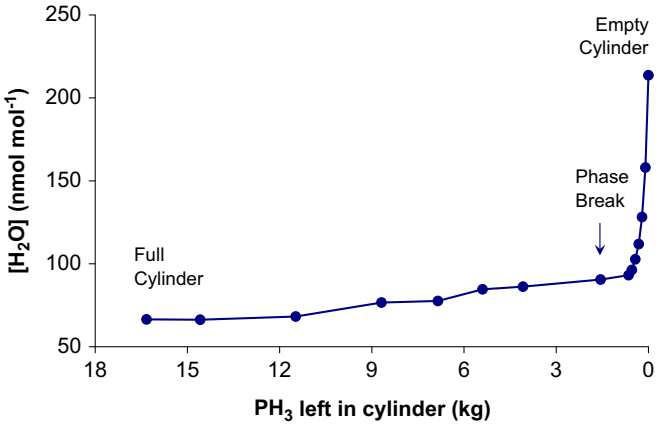

Fig. 7. H_2O concentration profile as PH_3 gas is withdrawn from a high-purity PH_3 cylinder from full to empty condition.

These results indicate that H_xPO_y contamination, can absorb H_2O if dry or release H_2O if wet. As shown in Fig. 4, release of H_2O into dry PH_3 can elevate the H_2O level in the delivered gas to μmol mol^{-1} levels. Therefore even though the gas source itself may be highly pure, the purity at point-of-use may be substantially lower and cause performance variations of III–V devices.

3.5. H_2O impurity generation by reaction of PH_3 with metal oxides

Another factor that may influence the purity of delivered PH_3 gas is the generation of H_2O by reaction of hydride gases with metal oxides on the exposed steel surfaces of the gas delivery system [20].

$$Fe_2O_3 + 2PH_3 \rightarrow 2FeP + 3H_2O \quad (1)$$

In this work we studied the trend in water vapor in PH_3 under stagnant conditions (no flow). Fig. 6 shows the build-up of H_2O in PH_3 is much higher than that in N_2 under the same static conditions. The H_2O increased from low nmol mol^{-1} levels to about 610 nmol mol^{-1} in PH_3 and 420 nmol mol^{-1} in N_2 after 36 h. After 48 h it increased to 1900 nmol mol^{-1} in PH_3 and 900 nmol mol^{-1} in N_2. In the N_2 case, the water is due to outgassing from the inner metal surfaces. In the case of PH_3, water not only continues to outgas but is also generated by reaction (1). The results show that in manifold design or use, it is important to keep process or purge gas under dynamic flow conditions rather than static conditions.

3.6. Water vapor profile during PH_3 gas consumption

Previous cylinder depletion studies on hydride gases have shown that gas phase H_2O can vary during gas withdrawal from the cylinder [3]. In this work we tracked the water vapor profile during depletion of a high-purity PH_3 cylinder (Fig. 7). The full cylinder (with ~16.33 kg PH_3) contained ~66 nmol mol^{-1} H_2O. From the full condition to liquid phase-break (~1.56 kg PH_3 left), the H_2O level remained approximately constant and below the 100 nmol mol^{-1} specification. As flow continued and the cylinder pressure finally dropped to ~137.9 kPa, the H_2O concentration increased to 214 nmol mol^{-1}. This result shows the importance of using a high-purity PH_3 source with low H_2O, switching out

cylinders in good time and/or the use of purification as discussed below, to ensure that water vapor is kept in control during III–V device fabrication.

Since water vapor can come from several sources and the delivery system may be difficult to purge and dry down due to the presence of even traces of H_xPO_y contamination, point-of-use purification is recommended close to the tool. A dry-down experiment with a $\sim$3 m delivery line showed that as Nanochem PHX purified PH_3 was introduced into the line, H_2O was reduced from 200 nmol mol^{-1} to single digit nmol mol^{-1} levels in $<$100 min.

4. Conclusion

Increasing mobility in InP films with run time has highlighted the importance of H_2O contamination issues in PH_3 delivery systems. The purity of delivered PH_3 is dependent on several factors. As with other gases, the source purity is important. Impurities such as H_2O may rise as gas is withdrawn from the cylinder, particularly close to or after phase-break. However additional issues exist for PH_3. Water may be generated by reaction of the PH_3 with surface metal oxides. Further H_xPO_y solids can slowly build up in delivery systems due to incomplete purging of atmospheric oxygen which reacts with the PH_3. H_2O can be emitted from these H_xPO_y solids and significantly lengthen dry-down times. To consistently control impurities, high-purity PH_3 and at-tool point-of-use purification is recommended.

Acknowledgement

We thank Markus Weyers and Carsten Netzel, FBH, Berlin, for practical help with the InP PL measurements

References

[1] J.W. Huang, J.M. Ryan, K.L. Bray, T.F. Kuech, J. Electron. Mater. 24 (1995) 1539.
[2] J.G. Cederberg, K.L. Bray, T.F. Kuech, J. Appl, Physics 82 (1997) 2263.
[3] J. Feng, R. Clement, M. Raynor, J. Crystal Growth 310 (2008) 4780.
[4] K.A. Bertness, S.R. Kurtz, S.E. Asher, R.C. Reedy Jr., J. Crystal Growth 196 (1999) 13.
[5] G.O. Munns, W.L. Chen, M.E. Sherwin, D. Knightly, G.I. Haddad, L. Davis, P.K. Bhattacharya, J. Crystal Growth 136 (1994) 166.
[6] A.J. Springthorpe, R.W. Streater, A. Joshi, US patent 6,653,213.
[7] N. Xiang, J. Likonen, J. Turpeinen, M.J. Saarinen, M. Toivonen, M. Pessa, Proc. SPIE 4086 (2000) 72.
[8] N. Iwata, T. Inoshita, Appl. Phys. Lett. 50 (1987) 1361.
[9] H.H. Funke, M.W. Raynor, K.A. Bertness, Y. Chen, Appl. Spectrosc. 61 (2007) 419.
[10] J. Feng, M. Raynor, Y. Chen, Compd. Semicond. 13 (2007) 31.
[11] W.M. Geiger, M.W. Raynor, Spectroscopy 23 (2008) 34.
[12] L.J. Van der Pauw, Philips Res. Rep. 13 (1958) 1.
[13] L. Pavesi, F. Piazza, A. Rudra, J.F. Carlin, M. Ilegems, Phys. Rev. B 44 (1991) 9052.
[14] W. Ruhle, W. Klingenstein, Phys. Rev. B 18 (1978) 7011.
[15] D.V. Shenai, M.L. Timmons Jr., R.L. DiCarlo, C.J. Marsman, J. Crystal Growth 272 (2004) 603.
[16] T. Watanabe, H.H. Funke, R. Torres, M.W. Raynor, V.J. Houlding, J. Crystal Growth 248 (2003) 67.
[17] R. Torres, T. Watanabe, J. Vininski, D. Lawrence, Z.H. Yang, W. Wang, J. Garcia, C.H. Yan, J. Crystal Growth 261 (2004) 231.
[18] E.H. Arbib, B. Elouadi, J.P. Chaminade, J. Darriet, J. Solid State Chem. 127 (1996) 350.
[19] J.W. Flora, L.E. Byers, S.E. Plunkett, D.L. Faustini, J. Agric. Food Chem. 54 (2006) 107.
[20] E. Flaherty, C. Herold, J. Wojciak, D. Murray, A. Amato, S. Thompson, Solid State Technol. 30 (1987) 69.